

1 2 3 4 1 **Transcriptional mapping of the primary somatosensory cortex upon sensory deprivation**

5
6 2 Koen Kole^{1,2}, Yutaro Komuro¹, Jan Provaznik³, Jelena Pistolic³,

7
8 3 Vladimir Benes³, Paul Tiesinga², Tansu Celikel¹

9
10 4 (1) Department of Neurophysiology, (2) Department of Neuroinformatics, Donders Institute for
11 5 Brain, Cognition, and Behaviour, Radboud University, Nijmegen - the Netherlands. (3) European
12 6 Molecular Biology Laboratory (EMBL), Genomics Core Facility, Heidelberg - Germany

13
14 7 E-mail addresses (in the order of appearance): k.kole@neurophysiology.nl,
15 8 y.komuro@neurophysiology.nl, jan.provaznik@embl.de, jelena.pistollic@embl.de,
16 9 benes@embl.de, p.tiesinga@science.ru.nl, celikel@neurophysiology.nl (corresponding author)

18 10 19 11 **Abstract**

20 12 Background: Experience-dependent plasticity (EDP) is essential for anatomical and functional
21 13 maturation of sensory circuits during development. Although the principal synaptic and circuit
22 14 mechanisms of EDP are increasingly well studied experimentally and computationally, its
23 15 molecular mechanisms remain largely elusive. EDP can be readily studied in the rodent barrel
24 16 cortex, where each 'barrel column' preferentially represents deflections of its own principal
25 17 whisker. Depriving select whiskers while sparing their neighbours introduces competition
26 18 between barrel columns, ultimately leading to weakening of intracortical, translaminar (i.e.
27 19 Cortical Layer (L)4-to-L2/3) feed-forward excitatory projections in the deprived columns. The
28 20 same synapses are potentiated in the neighbouring spared columns. These experience-
29 21 dependent alterations of synaptic strength are thought to underlie somatosensory map plasticity.
30 22 We used RNA sequencing in this model system to uncover cortical-column and -layer specific
31 23 changes on the transcriptome level that are induced by altered sensory experience.

32 24 Findings: Column- and layer-specific barrel cortical tissues were collected from juvenile mice
33 25 with all whiskers intact and mice that received 11-12 days long whisker (C-row) deprivation
34 26 before high quality RNA was purified and sequenced. The current dataset entails an average of
35 27 50 million paired-end reads per sample, 75 base pairs in length. On average, 90.15% of reads
36 28 could be uniquely mapped to the mm10 reference mouse genome.

37 29 Conclusions: The current data reveal the transcriptional changes in gene expression in the
38 30 barrel cortex upon altered sensory experience in juvenile mice and will help to molecularly map
39 31 the mechanisms of cortical plasticity.

40 32
41 33 **Keywords:** barrel cortex, RNA-sequencing, experience-dependent plasticity, whisker plucking,
42 34 sensory deprivation, transcriptomics

1
2
3
4
5
6
7
8
9
10
11
12
13
14
15
16
17
18
19
20
21
22
23
24
25
26
27
28
29
30
31
32
33
34
35
36
37
38
39
40
41
42
43
44
45
46
47
48
49
50
51
52
53
54
55
56
57
58
59
60
61
62
63
64
65

1
2
3
4
5
6
7
8
9
10
11
12
13
14
15
16
17
18
19
20
21
22
23
24
25
26
27
28
29
30
31
32
33
34
35
36
37
38
39
40
41
42
43
44
45
46
47
48
49
50
51
52
53
54
55
56
57
58
59
60
61
62
63
64
65

35 **Data Description**

36 **Context**

37 Sensory experience powerfully shapes neural circuits. Changes due to sensory organ deprivation
38 such as eye closure, digit amputation, and whisker trimming provide powerful means for studying
39 mechanisms of experience dependent cortical plasticity.

40 In the whisker system experience dependent plasticity is most commonly studied in the
41 barrel cortex subfield of the primary somatosensory cortex where neural representations of
42 whiskers change in response to altered patterns of incoming sensory information. As originally
43 shown in the barrel cortex [1] sensory deprivation induced by transient whisker trimming is
44 sufficient to perturb neural receptive fields both during development and in adulthood. Previous
45 work has also shown that the cellular basis of deprivation-induced decreases in whisker evoked
46 representations are primarily due to a reduction of synaptic strength in monosynaptically
47 connected feed-forward neuronal networks in behaving animals [2, 3]. Conversely whisker
48 sparing induced enhancement in whisker representation is mediated at least in part by the long-
49 term synaptic facilitation expressed along the L4 projections *in vivo* [4]. Identification of the
50 molecular events that mediate these bidirectional changes in synaptic connectivity will benefit
51 from systematic analysis of the gene transcription. Therefore, we performed RNA sequencing in
52 the barrel cortex with or without sensory deprivation across cortical layers 2-4. This database will
53 assist molecular and cellular neurobiologists in addressing the molecular mechanisms associated
54 with experience dependent plasticity, and will enable statistical approaches to determine the
55 dynamics of the coupled changes across molecular pathways as cortical circuits undergo plastic
56 changes in their organization.

57

1
2
3
4 58 **Methods**

5
6 59 *Animals*

7
8 60 All experiments were performed in accordance with the Animal Ethics Committee of the Radboud
9
10 61 University in Nijmegen, the Netherlands. Pregnant wild type mice (Charles River, stock number
11
12 62 000664) [RRID:NCBITaxon_10090] were kept at a 12-hour light/dark cycle with access to food
13
14 63 *ad libitum*. Cages were checked for birth daily. To induce experience-dependent plasticity, pups
15
16 64 underwent bilateral plucking of their C-row whiskers under isoflurane anaesthesia at P12 (**Figure**
17
18 65 **1**). Control animals were not plucked but anaesthetized and handled similarly. After recovery pups
19
20 66 were returned to their home cage. Every other day pups were checked for whisker regrowth,
21
22 67 which were plucked if present. At P23-P24, pups were randomly selected from their litter for slice
23
24 68 preparation and tissue collection. For each experimental condition (i.e. whisker deprived or
25
26 69 control), 4 female pups were used, thus each group consisted of 4 independent biological samples
27
28 70 (also known as biological replicates). Samples from cortical layer (L) 4 and L2/3 were treated
29
30 71 independently with their own corresponding groups of control, deprived, 1st order spared, 2nd order
31
32 72 spared columns as detailed in Figure 1.
33
34
35
36
37
38
39

40 74 *Figure 1 is about here*

41
42 75
43
44 76 *Slice preparation and sample collection*

45
46 77 Pups were anaesthetized using isoflurane and then perfused with ice-cold carbogenated slicing
47
48 78 medium (108 mM ChCl, 3 mM KCl, 26 mM NaHCO₃, 1.25 mM NaH₂PO₄, 25 mM glucose, 1 mM
49
50 79 CaCl₂, 6 mM MgSO₄ and 3 mM Na-pyruvate). Next, pups were decapitated before the brain was
51
52 80 quickly dissected out and 400 µm thalamocortical slices from each hemisphere were prepared as
53
54 81 described before [2, 3]. Slices were transferred to 37 degrees Celsius carbogenated ACSF (120
55
56 82 mM NaCl, 3.5 mM KCl, 10 mM glucose, 2.5 mM CaCl₂, 1.3 mM MgSO₄, 25 mM NaHCO₃ and 1.25
57
58
59
60
61
62
63
64
65

1
2
3
4 83 mM NaH₂PO₄) where they were kept for 30 minutes and recovered at room temperature for
5
6 84 another 30 minutes until tissue collection.
7

8
9 85

10 86 After incubation, slices were placed under a Nikon Eclipse FN1 microscope. The holding chamber
11
12
13 87 was continuously perfused with room temperature carbogenated ACSF. Due to the 55 degree
14
15 88 cut, slices were obtained in which S1 barrels from specific rows (A-E) could be identified [2]. A
16
17 89 thin, long glass pipette was pulled using a Sutter instruments P-2000 pipette puller and was used
18
19
20 90 to make intercolumnar incisions from L1 to the bottom of L4 after which the slice was placed under
21
22 91 a binocular dissection microscope where the location of specific barrel columns could now be
23
24 92 readily identified by eye. A sterile 32G needle was then used to cut out L2/3 and L4 separately
25
26 93 from each column. Tissue from columns A/E and B/D were pooled as they both constitute second
27
28 94 and first order spared whiskers, respectively. Immediately after dissection, tissue samples were
29
30 95 snap frozen in liquid nitrogen and stored at -80 degrees Celsius until further use. All tools that
31
32
33 96 came into direct contact with brain tissue were treated using RNaseZap in order to minimize
34
35 97 RNase contamination.
36

37
38 98

39 40 99 *RNA isolation and quality control*

41
42 100 Tissue samples originating from the same rows and layers were pooled within each animal. From
43
44 101 control animals, only the C column tissues were used (also see *Re-use potential*). Tissue was
45
46 102 quickly dissolved in Qiazol (Qiagen #79306), after which RNA was isolated using the miRNeasy
47
48
49 103 Mini kit (Qiagen #217004), DNase treated (Thermo Scientific, #EN0521) and cleaned up using
50
51 104 RNeasy MinElute kit (Qiagen #74204), all following the manufacturer's instructions. Samples were
52
53 105 then stored at -80 degrees Celsius until further processing.
54

55
56 106

57
58 107 RNA sample integrity was determined using Agilent Tapestation (High Sensitivity RNA
59
60 108 Screentape). Sample RINs ranged from 7.1 to 8.8. To further assess RNA purity and integrity,
61
62
63
64
65

1
2
3
4 109 RNA samples were used in RT-PCR to confirm that cDNA could be produced and that a large
5
6 110 (~1000 bp) amplicon could be obtained. To produce cDNA, SuperScript® II Reverse
7
8 111 Transcriptase (Thermo Scientific #18064014) and random hexamer primers (Roche
9
10 112 #11034731001) were used. The resulting cDNA was then added to a PCR reaction mix which
11
12
13 113 further consisted of Jumpstart Ready Mix (Sigma P2893) and exon-exon junction spanning
14
15 114 CamKII primers (FW TCCAACATTGTACGCCTCCAT; RV TGTTGGTGCTGTCGGAAGAT).
16
17 115 From all cDNA samples a fragment of the expected size could be amplified, suggesting that the
18
19 116 RNA samples contained pure RNA of sufficient integrity. All RNA samples thus passed our quality
20
21
22 117 control criteria and were subjected to RNA sequencing.
23

24 118 25 26 119 *RNA sequencing*

27
28 120 RNA sequencing was conducted at the Genomics Core Facility of the EMBL, Heidelberg,
29
30 121 Germany [RRID:SCR_004473]. The cDNA library was generated using the non-stranded
31
32 122 NEBNext Ultra RNA Library Preparation Kit for Illumina (New England Biolabs, catalogue
33
34 123 #E7530), which includes oligo-dT bead selection of mRNA. For library enrichment, 13-14 PCR
35
36 124 cycles were performed. Pooled libraries were sequenced on the Illumina NextSeq 500 instrument
37
38 125 [RRID:SCR_014983] in a 75bp paired-end mode using High output flow cells.
39

40 126 41 42 43 44 127 **Data validation and quality control**

45
46 128 Sequencing read quality was assessed using FastQC (Babraham Bioinformatics)
47
48 129 [RRID:SCR_014583], the results of which were merged using MultiQC (<http://multiqc.info>)
49
50 130 [RRID:SCR_014982]. Results are displayed in **Figure 2**. Per base quality *phred* scores range
51
52 131 from 34.80 to 35.15, indicating base call accuracies of >99.9% (**Figure 2A**). Overall 91.48-94.03%
53
54 132 of reads had a mean *phred* score of 30 or above (**Figure 2B**). In line with these scores, per base
55
56 133 N content (i.e. percentage of bases that could not confidently called) was very low, with a
57
58 134 maximum value 0.053%.
59
60
61
62
63
64
65

1
2
3
4
5
6
7
8
9
10
11
12
13
14
15
16
17
18
19
20
21
22
23
24
25
26
27
28
29
30
31
32
33
34
35
36
37
38
39
40
41
42
43
44
45
46
47
48
49
50
51
52
53
54
55
56
57
58
59
60
61
62
63
64
65

135

136

Figure 2 is about here

137

138

Reads were then mapped to the mm10 reference genome using STAR [5] [RRID:SCR_005622], which uniquely mapped between 39,000,000 and 59,000,000 reads, constituting an average 90.15% unique map rate across samples (**Figure 2D**). Since the library preparation protocol entails a PCR enrichment step, which can lead to technical duplication and hence an overestimation of observed transcripts, we used Seqmonk (Babraham Bioinformatics) [RRID:SCR_001913] to plot the read density against the duplication levels (i.e. the percentage of duplicate reads) for each transcript. The obtained duplication plots showed a clear positive relation between read density and duplication levels (**Figure 3** and **Supplemental Figure 1**), suggesting that the origin of read duplication is biological, rather than technical.

147

Based on the above quality control measures we determined that our RNA-sequencing data was of sufficient quality to be used in downstream analyses, therefore we continued with gene expression analysis.

150

Figure 3 is about here

151

152

153

Analysis of gene expression

154

Using a 2 read cut-off we identified 16,900 to 17,600 transcripts per sample (**Figure 4A**). Raw gene counts can be found online (see Supporting Data [6]). Differential gene expression analyses across groups were performed using EdgeR v3.12.1 [7, 8] [RRID:SCR_012802] using only genes with a count per million (CPM) >1 in at least 4 samples (**Supplementary Table 1** for details on the commands used). Since laminar identity is an important feature of our experimental setup, we assessed the relative expression of known molecular markers for L2/3 (*Cacna1h*, *Id2*, *Igfbp4*,

1
2
3
4 161 *Igfn1, Mdga1, Plcxd1, Rasgrf2, Rgs8, Tle3*) and L4 (*Cartpt, Cyp39a1, Kcnh5, Kcnip2, Lmo3,*
5
6 162 *Rorb, Scnn1a*) [9–11], which showed selective enrichment of the laminar markers in isolated
7
8 163 layers (**Figure 4B**).

10
11 164
12
13 165 *Figure 4 is about here*
14

15 166
16
17 167 To assess the variance in transcript counts, we calculated the coefficient of variation (CV) for
18
19 168 each transcript with a cut-off of 50 as the minimal read count separately for each group (**Figure**
20
21 169 **4C**). This analysis showed that, on average, 85.93% of transcripts have a CV below 15%,
22
23 170 suggesting low variance across transcript counts for individual genes. Principal component
24
25 171 analysis (PCA) showed that samples cluster based on layer, and the first two components
26
27 172 explained ~88% variance the data (**Figure 4C, Supplemental Figure 2B**).

28
29 173
30
31 174 These quality control routines suggest that we have obtained RNA-sequencing data of high read
32
33 175 quality, with individual bases being called confidently throughout the length of reads, which
34
35 176 uniquely map to the mm10 reference genome at high rates (>90% average). The laminar origin
36
37 177 of our samples could be identified through known molecular markers, confirming our samples are
38
39 178 of high anatomical specificity.
40
41
42
43

44 179 45 46 180 **Re-use potential**

47
48 181 The current RNA-seq dataset might help address the molecular underpinnings of cortical
49
50 182 experience-dependent plasticity. For example, it could be used (1) to identify genes whose
51
52 183 transcription is modulated in an experience-dependent manner, (2) to statistically map the
53
54 184 transcriptional networks at laminar resolution, (3) creating synergy with the single neuron RNA-
55
56 185 seq datasets [12, 13], to address the molecular diversity of the cortical networks, (4) combined
57
58 186 with the proteomic analysis performed under comparable experimental conditions in the
59
60
61
62
63
64
65

1
2
3
4
5
6
7
8
9
10
11
12
13
14
15
16
17
18
19
20
21
22
23
24
25
26
27
28
29
30
31
32
33
34
35
36
37
38
39
40
41
42
43
44
45
46
47
48
49
50
51
52
53
54
55
56
57
58
59
60
61
62
63
64
65

187 accompanying manuscript (Kole et al, submitted), to systematically study the transcriptional and
188 translational regulation of the genome upon altered sensory experience, and finally (5) to identify
189 and quantify splice isoforms, given the sequencing depth of the current dataset. Since splicing
190 and other posttranscriptional mechanisms govern which proteins are ultimately produced,
191 combining the current transcriptomic dataset with a proteomics approach [14] would also be of
192 high importance.

193

194 The current dataset focuses on isolated cortical columns and layers, which are necessarily
195 diverse samples containing neuronal and non-neuronal cell classes. In terms of experience
196 dependent plasticity, although most previous studies focus on excitatory projections, inhibitory
197 cells and even non-neuronal cells have been implicated in plasticity [15–17]. This heterogeneity
198 might be particularly important for L2/3, as also shown by the principal component analysis
199 (**Figure 4D**), given the relative diversity of cellular populations in supragranular layers and their
200 heterogeneous connectivity patterns [18].

201

202 Researchers reusing our dataset should be aware that comparisons between control column C
203 and spared columns (A/E, B/D) may have to be approached with caution, as this would involve
204 two different columnar identities (whose transcriptomic dissimilarities are currently unknown),
205 each coming from cortices that have had different sensory experience. However direct
206 comparisons between the C columns across experimental conditions (i.e control versus deprived)
207 as well as within-animal across-column comparisons in deprived animals control for these
208 confounding variables.

209

210 Taken together we hope that this data will prove useful in discovering novel molecular targets
211 responsible for cortical plasticity and will lead to targeted control of plasticity in health and disease.

212

1
2
3
4
5
6
7
8
9
10
11
12
13
14
15
16
17
18
19
20
21
22
23
24
25
26
27
28
29
30
31
32
33
34
35
36
37
38
39
40
41
42
43
44
45
46
47
48
49
50
51
52
53
54
55
56
57
58
59
60
61
62
63
64
65

213 Availability of the supporting data

214 All supporting data are available in the GigaScience repository, GigaDB [6].
215 The raw sequence reads were deposited in the NCBI under GEO accession GSE90929

217 List of abbreviations

218 EDP Experience dependent plasticity
219 L2/3 Cortical Layer 2/3, also known as supragranular layers
220 L4 Cortical Layer 4, i.e. granular layer

222 Competing interests

223 The authors declare that they have no competing interests.

225 Funding

226 Funding for the current work was provided by the Faculty of Science of the Radboud University,
227 Nijmegen, the Netherlands (grant number 626830 – 6200821) as well as the ALW Open
228 Programme of the Netherlands Organization for Scientific Research (NWO; grant number
229 824.14.022).

231 Author contributions

232 KK performed all experimental manipulations, sample acquisition, biological and bioinformatic
233 quality controls, and prepared the tables and figures. YK and JaP performed bioinformatic
234 analysis. JeP performed library prep. VB supervised RNA-seq. PT contributed bioinformatic
235 analysis and co-supervised the project. TC designed and supervised the project. KK and TC
236 wrote the manuscript. All authors edited otherwise approved the final version of the manuscript.

References

1. Hand PJ (1892) Plasticity of the rat cortical barrel system. In: Strick P, Morrison AD (eds) *Changing concepts of the nervous system*. Academic Press, New York, pp 49–75
2. Allen CB, Celikel T, Feldman DE (2003) Long-term depression induced by sensory deprivation during cortical map plasticity in vivo. *Nat Neurosci* 6:291–9. doi: 10.1038/nn1012
3. Celikel T, Szostak VA, Feldman DE (2004) Modulation of spike timing by sensory deprivation during induction of cortical map plasticity. *Nat Neurosci* 7:534–41. doi: 10.1038/nn1222
4. Clem RL, Celikel T, Barth AL (2008) Ongoing in vivo experience triggers synaptic metaplasticity in the neocortex. *Science* 319:101–4. doi: 10.1126/science.1143808
5. Dobin A, Davis CA, Schlesinger F, Drenkow J, Zaleski C, Jha S, Batut P, Chaisson M, Gingeras TR (2013) STAR: ultrafast universal RNA-seq aligner. *Bioinformatics* 29:15. doi: 10.1093/bioinformatics/bts635
6. Kole K, Komuro Y, Provaznik J, Pistolic J, Benes V, Tiesinga P, Celikel T: Supporting data for "Transcriptional mapping of the primary somatosensory cortex upon sensory deprivation". GigaScience Database. 2017. <http://dx.doi.org/10.5524/100296>
7. Robinson MD, McCarthy DJ, Smyth GK (2010) edgeR: a Bioconductor package for differential expression analysis of digital gene expression data. *Bioinformatics* 26:139. doi: 10.1093/bioinformatics/btp616
8. McCarthy DJ, Chen Y, Smyth GK (2012) Differential expression analysis of multifactor RNA-Seq experiments with respect to biological variation. *Nucleic Acids Res* 40:4288. doi: 10.1093/nar/gks042
9. Molyneaux BJ, Goff LA, Rinn JL, Arlotta P (2015) Genome-wide Analysis of In Vivo Transcriptional Dynamics during Pyramidal Neuron Fate Selection in Neocortex NeuroResource DeCoN: Genome-wide Analysis of In Vivo Transcriptional Dynamics during Pyramidal Neuron Fate Selection in Neocortex. 275–288.
10. Xue M, Atallah B V., Scanziani M (2014) Equalizing excitation–inhibition ratios across visual cortical neurons. *Nature* 511:596–600. doi: 10.1038/nature13321
11. Rowell JJ, Mallik AK, Dugas-Ford J, Ragsdale CW (2010) Molecular analysis of neocortical layer structure in the ferret. *J Comp Neurol* 518:3272–3289. doi: 10.1002/cne.22399
12. Zeisel A, Munoz-Manchado AB, Codeluppi S, Lonnerberg P, La Manno G, Jureus A, Marques S, Munguba H, He L, Betsholtz C, Rolny C, Castelo-Branco G, Hjerling-Leffler J, Linnarsson S (2015) Cell types in the mouse cortex and hippocampus revealed by single-cell RNA-seq. *Science* (80-) 347:1138–1142. doi: 10.1126/science.aaa1934
13. Tasic B, Menon V, Nguyen TN, Kim TK, Jarsky T, Yao Z, Levi B, Gray LT, Sorensen SA, Dolbeare T, Bertagnoli D, Goldy J, Shapovalova N, Parry S, Lee C, Smith K, Bernard A, Madisen L, Sunkin SM, Hawrylycz M, Koch C, Zeng H (2016) Adult mouse cortical cell taxonomy revealed by single cell transcriptomics. *Nat Neurosci* 19:335–346. doi: 10.1038/nn.4216
14. Kole K, Lindeboom RGH, Baltissen MPA, Jansen PWTC, Vermeulen M, Tiesinga P, Celikel T. Proteomic landscape of the primary somatosensory cortex upon sensory deprivation. *GigaScience*. 2017 (In Press)
15. Tropea D, Van Wart A, Sur M (2009) Molecular mechanisms of experience-dependent plasticity in visual cortex. *Philos Trans R Soc Lond B Biol Sci* 364:341–55. doi: 10.1098/rstb.2008.0269
16. Kole K (2015) Experience-dependent plasticity of neurovascularization. *J Neurophysiol* 114:2077–9. doi: 10.1152/jn.00972.2014
17. Foeller E, Celikel T, Feldman DE (2005) Inhibitory sharpening of receptive fields

1
2
3
4
5
6
7
8
9
10
11
12
13
14
15
16
17
18
19
20
21
22
23
24
25
26
27
28
29
30
31
32
33
34
35
36
37
38
39
40
41
42
43
44
45
46
47
48
49
50
51
52
53
54
55
56
57
58
59
60
61
62
63
64
65

287 contributes to whisker map plasticity in rat somatosensory cortex. *J Neurophysiol*
288 94:4387–400. doi: 10.1152/jn.00553.2005

18. Markram H, Muller E, Ramaswamy S, Reimann MW, Abdellah M, Sanchez CA, Ailamaki
289 A, Alonso-Nanclares L, Antille N, Arsever S, Kahou GAA, Berger TK, Bilgili A, Buncic N,
290 Chalimourda A, Chindemi G, Courcol J-D, Delalandre F, Delattre V, Druckmann S,
291 Dumusc R, Dynes J, Eilemann S, Gal E, Gevaert ME, Ghobril J-P, Gidon A, Graham JW,
292 Gupta A, Haenel V, Hay E, Heinis T, Hernando JB, Hines M, Kanari L, Keller D, Kenyon
293 J, Khazen G, Kim Y, King JG, Kisvarday Z, Kumbhar P, Lasserre S, Le Bé J-V,
294 Magalhães BRC, Merchán-Pérez A, Meystre J, Morrice BR, Muller J, Muñoz-Céspedes
295 A, Muralidhar S, Muthurasa K, Nachbaur D, Newton TH, Nolte M, Ovcharenko A,
296 Palacios J, Pastor L, Perin R, Ranjan R, Riachi I, Rodríguez J-R, Riquelme JL, Rössert
297 C, Sfyraakis K, Shi Y, Shillcock JC, Silberberg G, Silva R, Tauheed F, Telefont M, Toledo-
298 Rodriguez M, Tränkler T, Van Geit W, Díaz JV, Walker R, Wang Y, Zaninetta SM,
299 DeFelipe J, Hill SL, Segev I, Schürmann F (2015) Reconstruction and Simulation of
300 Neocortical Microcircuitry. *Cell* 163:456–492. doi: 10.1016/j.cell.2015.09.029
301
302

1
2
3
4 303
5
6
7
8
9
10
11
12
13
14
15
16
17
18
19
20
21
22
23
24
25
26
27
28
29
30
31
32
33
34
35
36
37
38
39
40
41
42
43
44
45
46
47
48
49
50
51
52
53
54
55
56
57
58
59
60
61
62
63
64
65

1
2
3
4 304 **Figure Legends**

5 305
6
7 306 **Figure 1.** Overview of the experimental design, sample collection and data organization. **(A)** Pups
8 307 were bilaterally spared or deprived of off their C-row whiskers between P12 and P23-P24, when
9 308 acute slices are made and column- and layer-specific tissues were excised. **(B)** RNA was isolated,
10 309 checked for integrity and purity, and subsequently sequenced. **(C)** Organization of the database.
11 310 Colour codes denote experimental groups. Same denominations are used in the read counts
12 311 matrix file (see **Supplemental Data**).
13 312

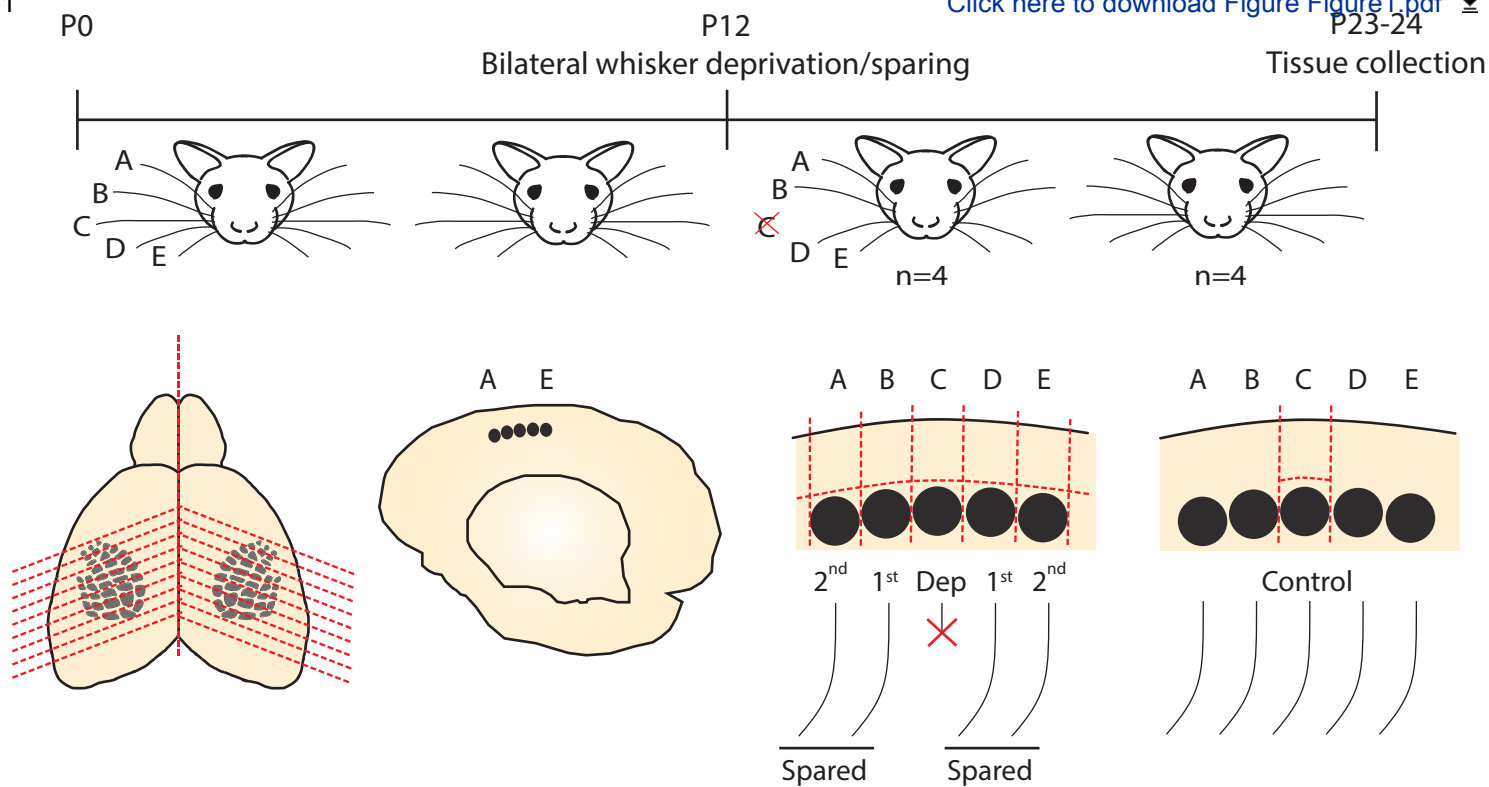
14
15 313 **Figure 2.** FastQC and STAR output graphs for all samples. **(A-B)** *Phred* scores per base and
16 314 per sequence. **(C)** Per sequence GC content. **(D)** STAR output of alignment scores.
17 315

18 316 **Figure 3.** Overlays of duplication plot contours, showing a positive correlation between read
19 317 density and duplication levels. Depicted contours enclose 90% of the data points.
20 318

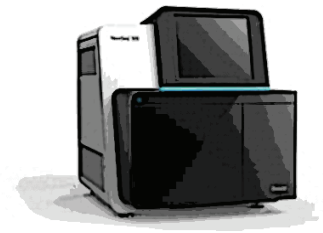
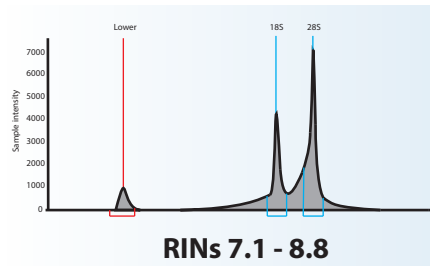
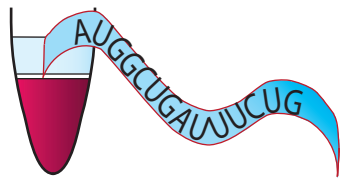
21
22 319 **Figure 4.** Gene expression analyses. **(A)** Histogram of read counts per transcript per sample.
23 320 With a cut-off of 2 reads, between 16,900 and 17,600 transcripts could be identified across
24 321 samples. **(B)** Relative expression of known molecular markers for cortical laminae. Layer 4
25 322 markers are enriched in samples originating from this layer; the same is true for Layer 2/3 marker
26 323 expression in Layer 2/3 samples. **(C)** Cumulative plots of the coefficient of variance (CV) of
27 324 individual experimental groups. Including only transcripts identified by 50 reads or more, average
28 325 CVs of <15% are found in ~85% of transcripts. **(D)** Principal component analysis (PCA) showing
29 326 sample clustering by layer, including only transcripts identified by at least 50 reads. Principal
30 327 component (PC) 1 and 2 account for 88% of overall variance.
31 328

32
33 329 **Supplemental Figure 1.** Duplication plots for all samples, produced using SeqMonk (Babraham
34 330 Bioinformatics).
35 331

36 332 **Supplemental Figure 2.** **(A)** Cumulative plots of the coefficient of variance (CV) of experimental
37 333 each group, including transcripts identified by at least one read. Average CVs of <25% are
38 334 found in ~85% of transcripts. **(B)** Principal component analysis (PCA) including transcripts
39 335 identified by at least one read. The majority (88%) of overall variance is explained by Principal
40 336 components (PC) 1 and 2.
41
42
43
44
45
46
47
48
49
50
51
52
53
54
55
56
57
58
59
60
61
62
63
64
65



B



RNA isolation, quality control and sequencing

C

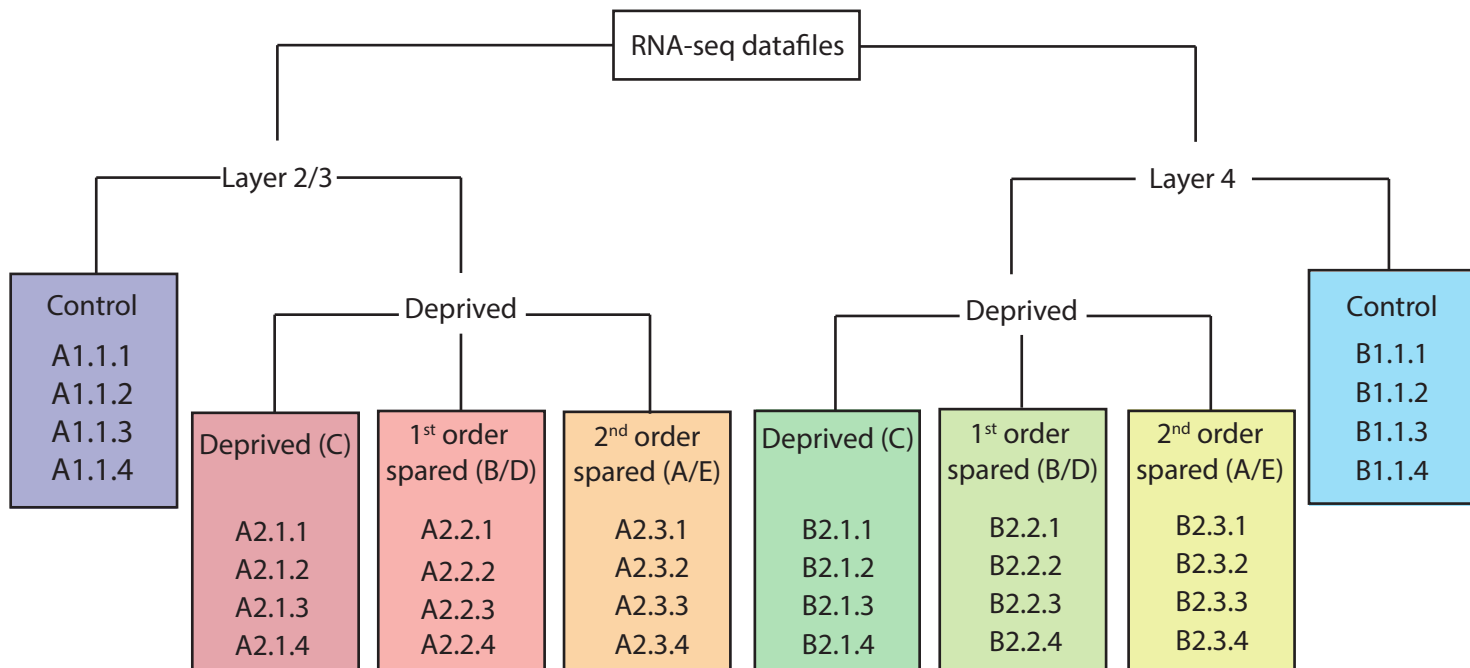


Figure2

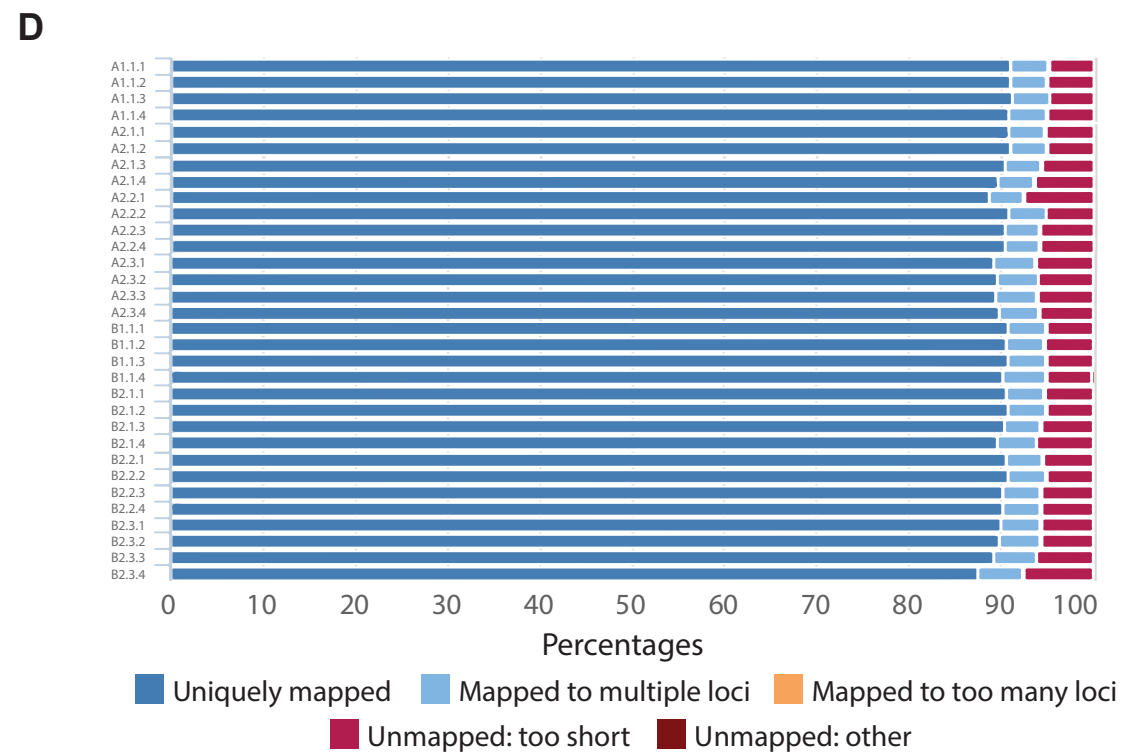
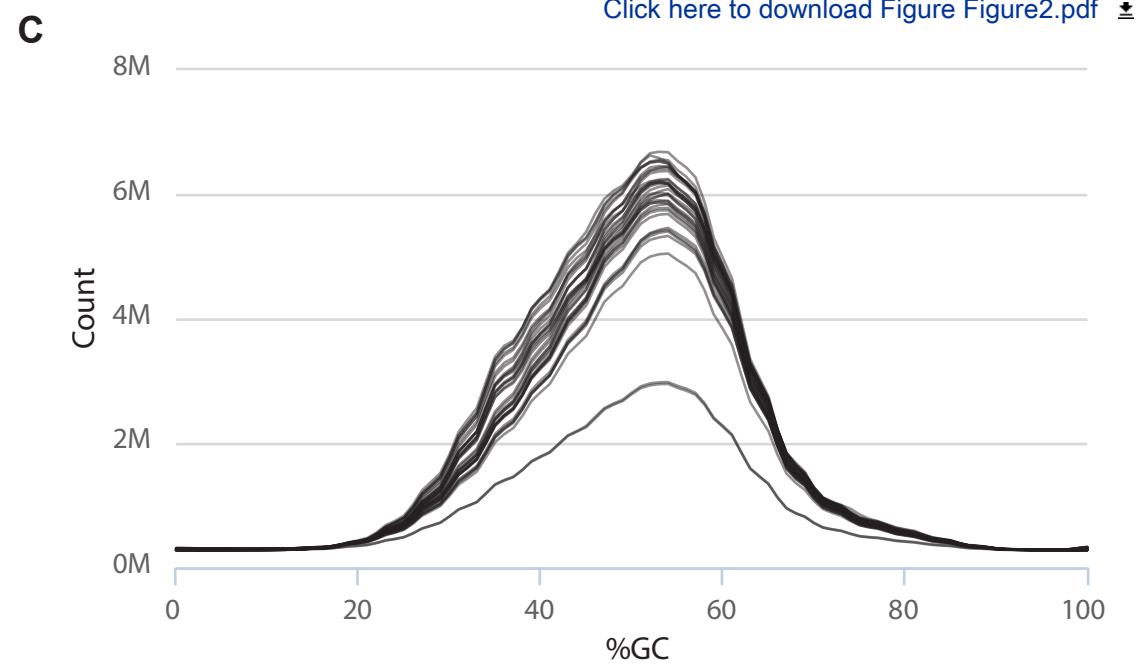
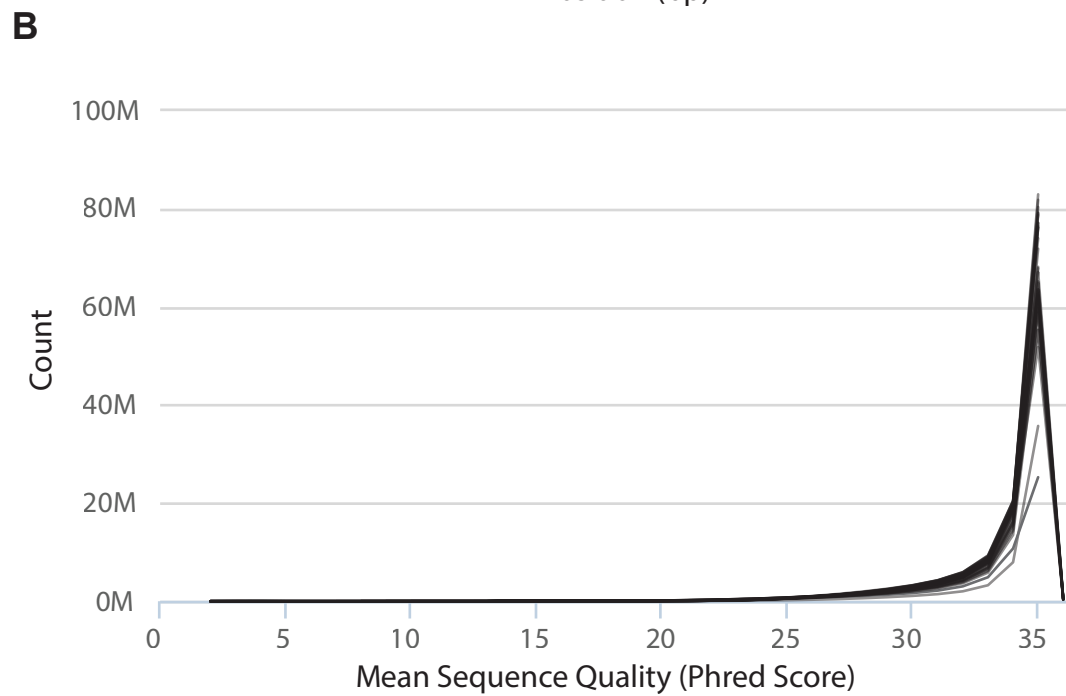
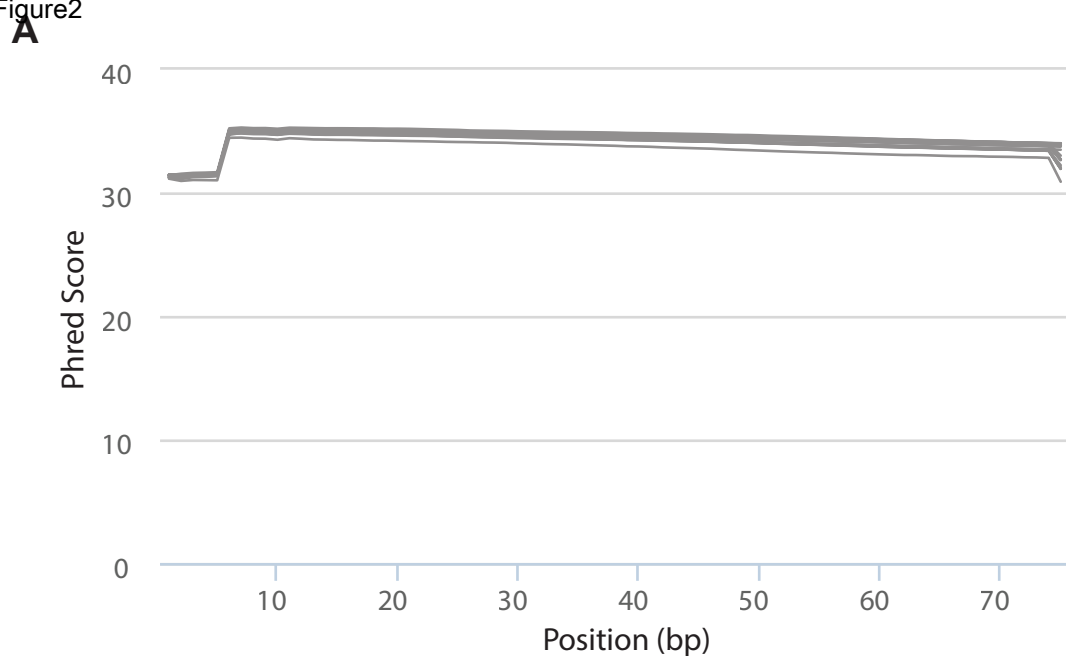


Figure3

[Click here to download Figure Figure3.pdf](#)

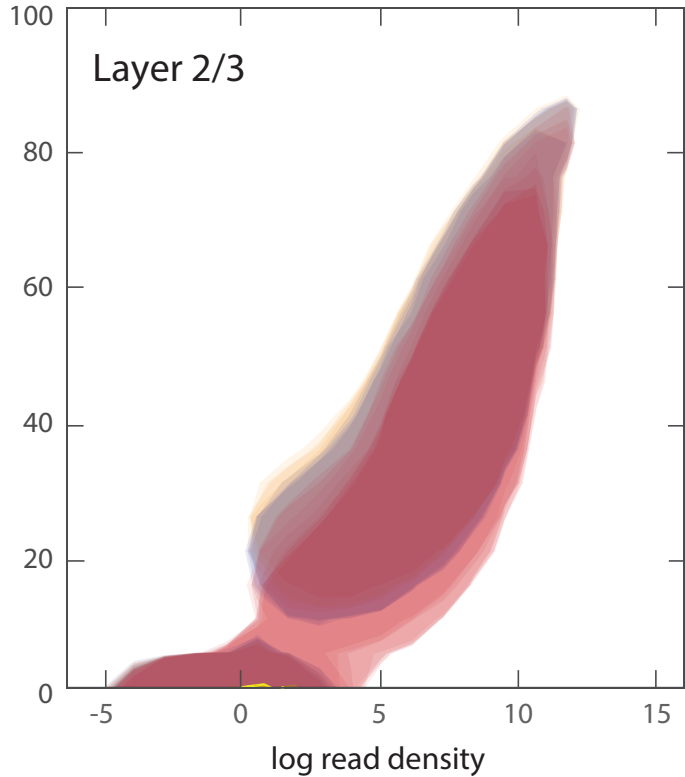
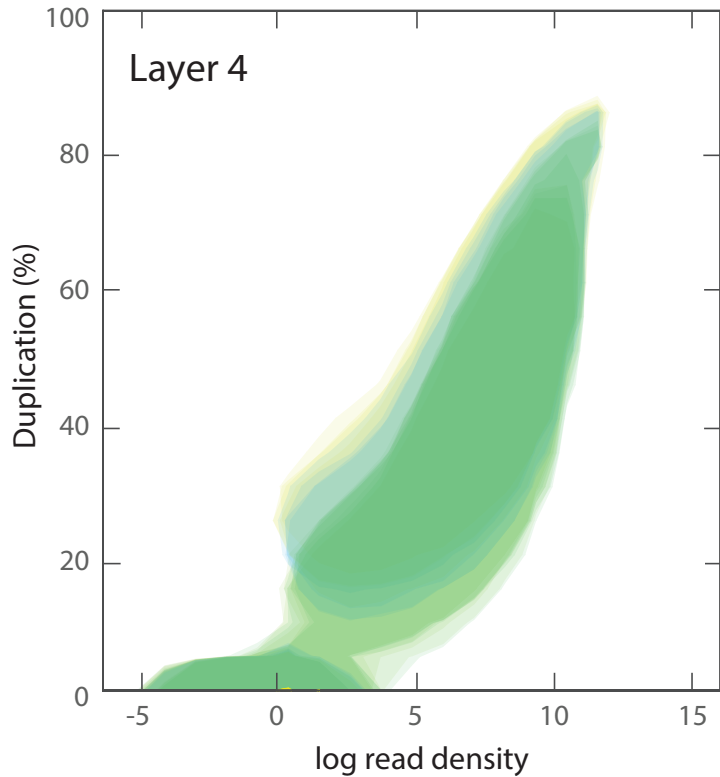
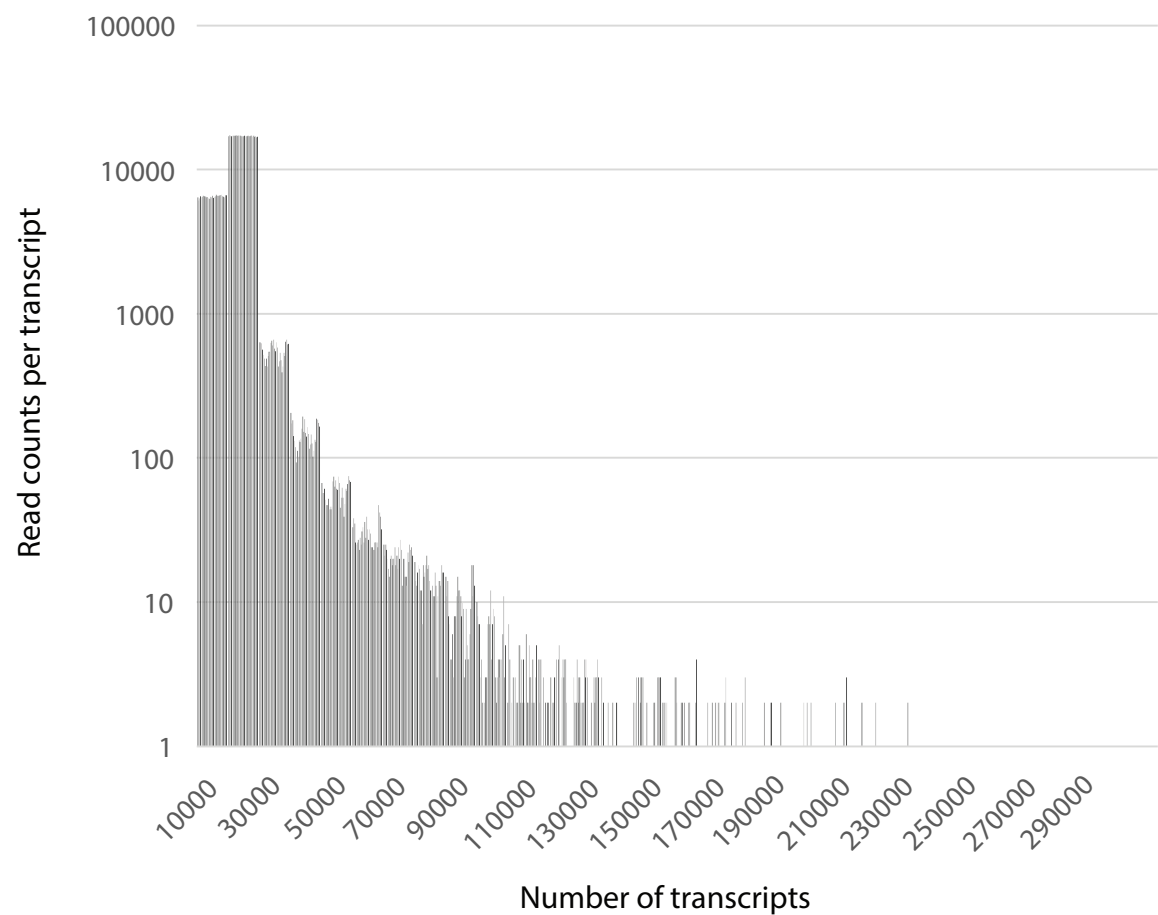
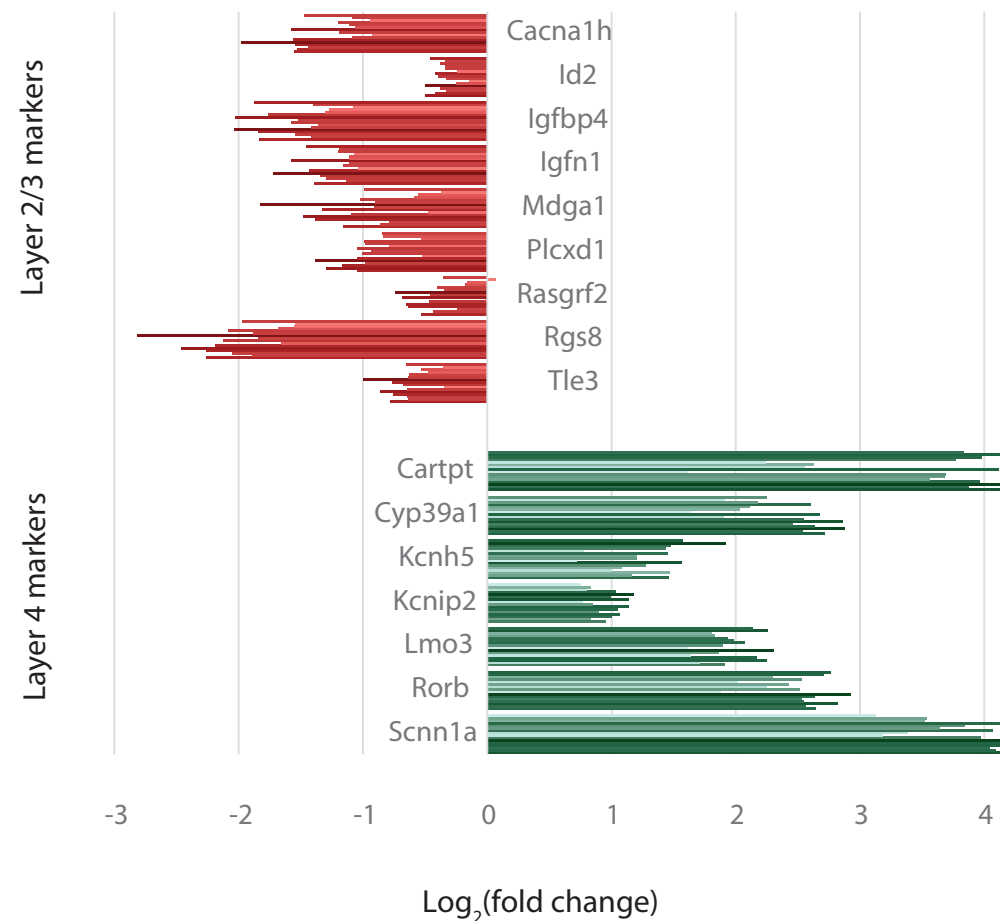
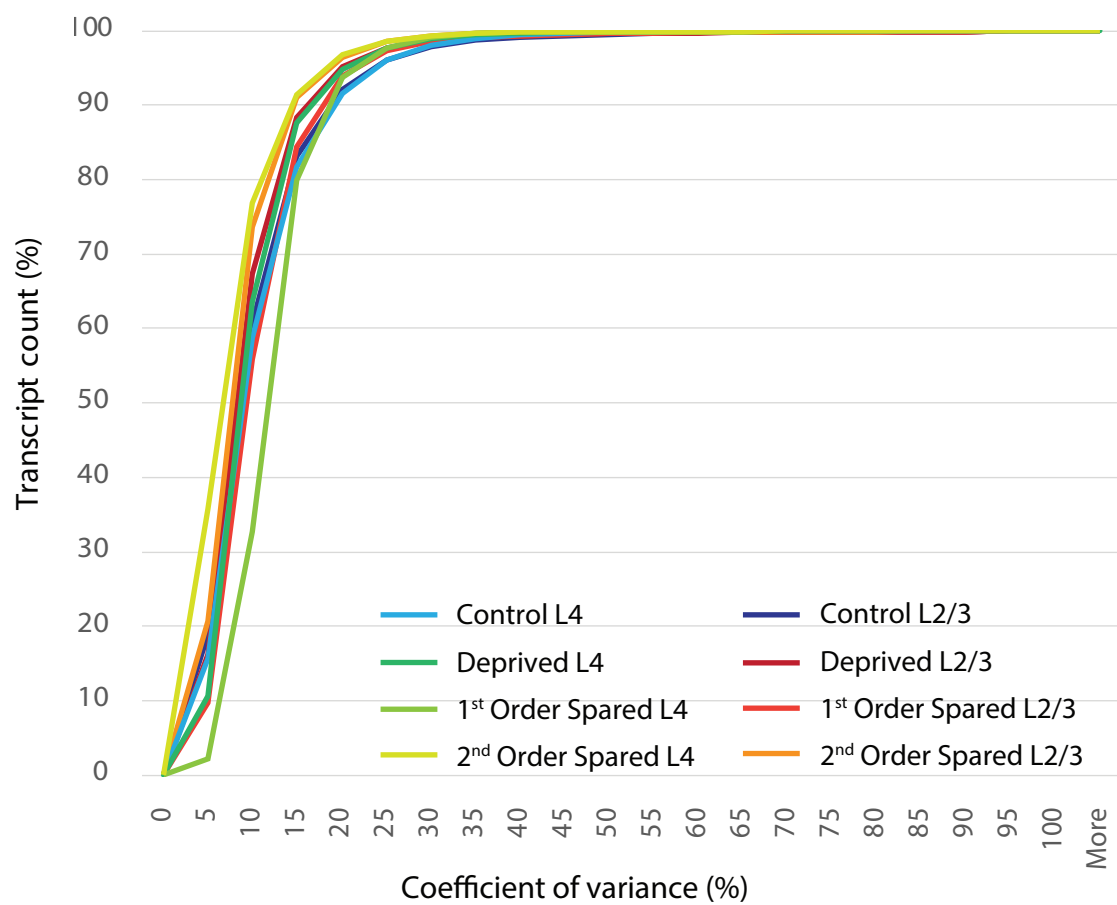
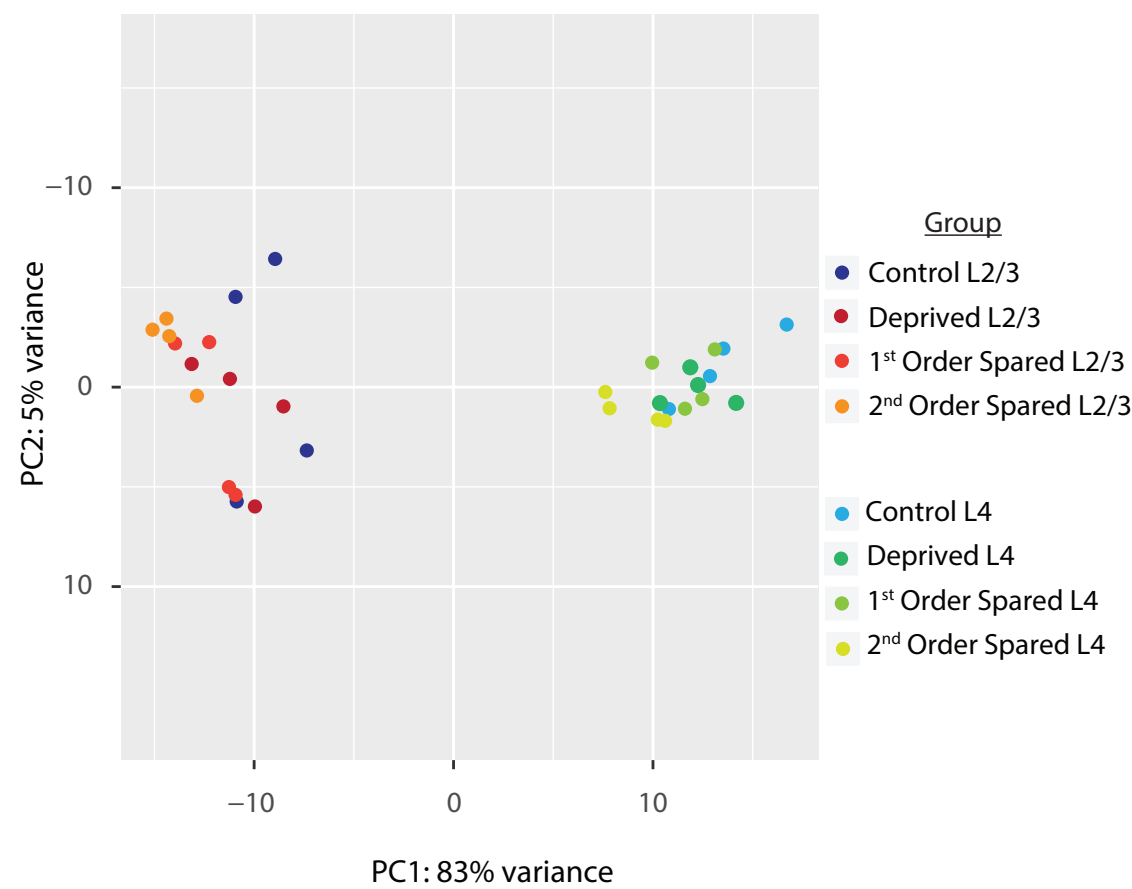


Figure 4

[Click here to download Figure Figure_4.pdf](#)**A****B****C****D**





[Click here to access/download](#)

Supplementary Material

[Supplementary_Table1_EdgeRcommands.txt](#)

